Welded, sandblasted, stainless steel corrugated bars in non-carbonated and carbonated mortars: A 9-year corrosion study

A. Bautista *, E.C. Paredes, S.M. Alvarez, F. Velasco

Material Science and Engineering Department, Universidad Carlos III de Madrid, Avda. Universidad n° 30., 28911 Leganés, Madrid, Spain

A B S T R A C T

Three different stainless steel corrugated grades (UNSS20430, S30403 and S32205) were similar welded to stainless steel bars with the same composition and dissimilar welded to carbon steel (CS).After cleaning the welding oxides by sandblasting, the reinforcements were embedded in mortar with chlorides and some of the samples were carbonated. Corrosion activity was monitored using corrosion potential (E_{corr}) and electrochemical impedance spectroscopy (EIS). After 8 years of exposure, the samples were anodically polarized. Visual evaluation of the attack was performed after another additional year of exposure. Similar welded stainless steels offer a good durability if they have been sandblasted, except for S20430 when it is embedded in carbonated mortar with chlorides. Dissimilar welded steels are active since the beginning of the exposure for both studied conditions, but sandblasting reduces the corrosion rate of CS compared to non-welded CS bars.

Keywords:
A. Stainless steel
A. Steel reinforced concrete
B. EIS
B. Polarization
C. Welding

1. Introduction

Stainless steel reinforcements are increasingly being used as an alternative to guarantee the durability of concrete structures in corrosive environments. The alkalinity of the solution inside the pores favors the protective nature of the oxides comprised in the passive layer of the stainless steels [1–3] and reduces the risk of localized corrosion in chloride-contaminated environments [4,5].

The typical forming process of corrugated bars causes microstructural transformations in the stainless steels [6,7]. The microstructural characteristics of the reinforced bars explains the decrease of the corrosion resistance in simulated pore solutions that has been detected for stainless steels when they are corrugated [8]. The mechanical strain of the surface causes a negative effect on the stoichiometry, composition and protective nature of the passive layer on the stainless steels [9]. However, the critical chloride levels that cause pitting corrosion in corrugated austenitic and duplex stainless steels are at least 10 times higher than those of carbon steel (CS) reinforcements [10], so they are an interesting alternative to prevent corrosion problems in reinforced concrete structures.

For economical reasons, stainless steel reinforcements are only used in the most exposed areas of new structures. For instance, they could be used in bridge parts like edge beams, expansion joint sections, piers and piers tops and bridge deck soffits. That is to say, areas where the environmental chlorides would penetrate, or carbonation would take place in shorter times, as they are close to concrete surface. Welding is not the most usual method for joining reinforcing bars, but it can be the only option sometimes. Welded mesh reinforcement of stainless steel are being used extensively, both for new constructions like parking decks etc, but also in repairs of reinforced concrete (especially when the concrete cover is thin).

It has been proved that the simultaneous use of stainless steel and CS reinforcements in the same structure does not imply any risk of galvanic corrosion [10–12]. Moreover, stainless steel corrugated bars are also used to repair corroded structures, as replacements of old, damaged CS bars [13,14]. When stainless steel bars are employed to replace part of corroded CS bars, it is sometimes unavoidable to weld the stainless steel reinforcements to the rest of the structure. As constructing new concrete infrastructures implies a high amount of CO_2 emissions, boosting the repair of damaged concrete infrastructures is nowadays seen as a new way to contribute to sustainable development [15]. The use of stainless steel reinforcement in repairs avoids future restoring actions in the structure. Hence, it is interesting to achieve a good knowledge about the effect of welding on the durability of stainless steel reinforcements in concrete.

The microstructural changes in metal bars caused by welding do not endanger the mechanical performance of the structure [16]. However, tests in alkaline solutions have pointed out that welding

* Corresponding author. Fax: +34 91 624 9430.
E-mail address: mbautist@ing.uc3m.es (A. Bautista).

can decrease the corrosion resistance of stainless steels [10–17]. Previous research carried out in simulated pore solutions suggests that the adverse effect of weldings can be more or less marked depending on the stainless steel grade: more alloyed stainless steels seem to be less welding-sensitive [17]. The pH of the alkaline solution has also proved to be a key factor to determine the corrosion resistance of welded stainless steel [18].

Solution tests have shown that the decrease in the corrosion resistance of stainless steels caused by welding is due to the formation of heat-tints during the high-temperature exposure that implies the welding procedure [4,19]. The causes suggested in the literature to justify the adverse effect of the heat-tints on corrosion behavior are diverse: formation of a Cr-poor layer [4], the chemical composition of the heat-tints [20], or the structure of the formed oxide layer and the stresses and reticular defects created in the metal–oxide interface [21].

Removing welding oxides after welding can improve corrosion resistance, but it can unlikely be restored up to levels of a non-welded corrugated stainless steel [17]. The comparative effectiveness of various methods used for cleaning the welding oxides has been reported, and sandblasting has been proposed as the most adequate method to decrease the adverse effect of welding in corrosion resistance [17].

In this work, the effect of welding in 3 different corrugated stainless steels in mortar is studied: an austenitic UNS S30403 grade (the composition with the longest and widest experience about its behavior in concrete [22,23]), an austenitic UNS S20430 grade (that has been considered interesting because of its price and its moderate corrosion resistance in synthetic pore solution testing [5,24]) and a duplex UNS S32205 grade (that has shown very high corrosion resistance in previous tests [1,25]). The 3 corrugated stainless steels were welded to similar materials and to CS bars, their welding oxides were cleaned by sandblasting, and then they were embedded in mortar and exposed to high relative humidity (90–93%). A chloride contaminated mortar was used, both non-carbonated and carbonated.

The length of the tests and the fact that they were carried out in mortar instead of in solution highlight the practical relevance of the results. The process of formation of the passive layer on steel in simulated pore solutions takes place faster than in mortar [26], so the passivation of welded stainless steels can also be slightly different from previous results in solution [17]. Moreover, if corrosion starts, there are important factors affecting the kinetic of the attack that can not be reproduced in solution tests [27].

2. Experimental

Samples of traditional austenitic S30403, low-Ni austenitic S20430 and duplex S32205 stainless steels were studied. The material was supplied by Roldan S.A. (Acerinox group, Spain) as corrugated bars typically used to reinforce concrete structures. All the stainless steel bars had been formed through a cold working process. The chemical composition and diameter of the stainless steel bars can be found in Table 1.

The stainless steel corrugated bars were similar welded to bars of the same composition (S30403–S30403, S20430–S20430 and S32205–S32205) and dissimilar welded to CS bars (S30403-CS, S20430-CS and S32205-CS). The diameters of the CS bars were always identical to those of the stainless steel bars they were going to be welded to. Their chemical compositions can be seen in Table 1.

The chosen welding method was Shielded Metal Arc Welding (SMAW) which is easily implementable in construction. The applied voltage was between 50 and 60 V, and the applied current was between 45 and 90 A. The welding electrode was OK 61.30 (UNS S30803 with a low-moisture absorption coating) for the austenitic steels and OK 67.50 (UNS S32209 with a rutile coating) for the duplex steel. The composition of the stainless steel welding electrodes and their diameters have also been included in Table 1. These welding conditions were similar to those used in previous researches in the performance of welded stainless steel reinforcements [16,17].

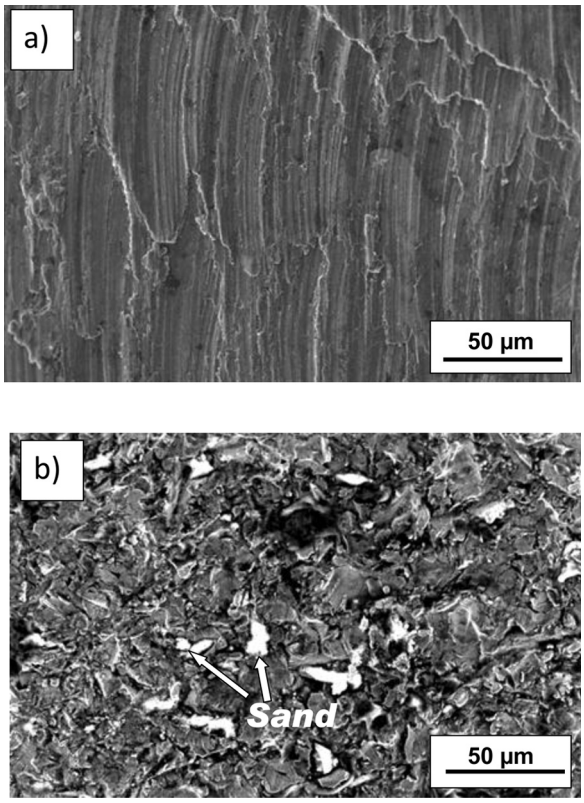

Fig. 1. SEM images corresponding to the surface of S20430 corrugated bar: (a) as-received condition; (b) after sandblasting.

All the welded samples were sandblasted to remove heat-tints. This treatment eliminated all the welding oxides formed on the stainless steel surfaces. However, it clearly modified the original topography of the bar surface, as can be checked comparing Fig. 1a with Fig. 1b. Moreover, some sand particles remained embedded in the metallic surface, as can also be seen in Fig. 1b.

The welded bars were partly immersed in mortar with a cement/sand/water ratio of 1/3/0.6. The water/cement ratio was high, as it is quite usual in experimental tests [13,27–29]. Bearing in mind that a good quality concrete can have a water/cement ratio of about 0.4, the use of this mortar samples will imply that the volume fraction of capillary porosity will be about 2 times higher after the curing period than that of good quality material [30], and nearly 3 times higher after the complete hydration of the cement [30]. However, this type of samples allows to obtain results in a reasonable period of time and can reproduce one of the conditions the stainless steel reinforcements are specially advised: light, porous concrete coatings. The cement type used to prepare the mortar was CEM II/B-L 32.5 N. The sand was standardized CEN-NORMSAND (according to the DIN EN 196-1 standard). All the samples were manufactured with 3% $CaCl_2$ in relation to the cement weight.

A schema of the samples is shown in Fig. 2. Isolating tape was used to prevent the interference of undesired, spontaneous carbonation of the mortar surface in the tests. The exposed length of the bar in mortar was always 3 cm and the welding was placed just in the middle of the length of the bar exposed to the mortar. For dissimilar welded reinforcements, the CS region was always

Table 1
Chemical composition and diameter of the corrugated steels and the welding electrodes used in this research.

Steel		Ø (mm)	Chemical composition (%)									
			S	C	Si	Mn	Cr	*Ni*	Mo	N	Cu	Fe
Corrugated bars	S20430	5	0.002	0.05	0.23	8.3	16.1	1.89	–	0.13	2.65	Bal.
	S30403	10	0.001	0.02	0.36	1.45	18.3	8.68	0.27	0.05	0.49	Bal.
	S32205	12	0.001	0.03	0.39	1.67	22.5	4.72	3.22	0.17	0.24	Bal.
	CS	5	0.03	0.25	0.74	1.05	0.23	0.07	0.02	–	0.66	Bal.
		10	0.03	0.18	0.40	0.53	0.10	0.11	0.04	–	0.45	Bal.
		12	0.04	0.21	0.39	0.04	0.13	0.09	0.02	–	0.42	Bal.
Welding wires	S30803	2.0	0.003	0.01	0.50	0.9	18.5	10.0	–	–	0.25	Bal.
	S32209	2.5	0.002	0.02	0.50	0.9	22.3	8.5	3.5	0.17	–	Bal.

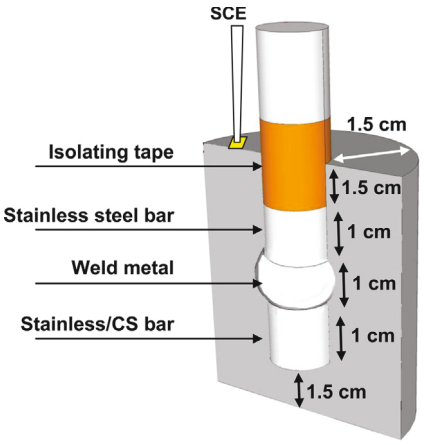

Fig. 2. Schema of the samples with welded reinforcements tested in the present research.

completely embedded in the mortar while the stainless steel region was placed in the top part of the samples. In half of the samples, an activated Ti-electrode was embedded close to the reinforcement.

After their manufacturing, the reinforced samples were cured for 30 days at high relative humidity (92–93%). Then, the samples with activated Ti-electrode were carbonated. The carbonation process was carried out in a chamber where 10% CO_2-enriched air was injected. The temperature in the chamber was $18 \pm 1\,^{\circ}C$ and the relative humidity was 75–80%. The potential of the Ti-electrode was monitored periodically using a saturated calomel electrode (SCE) placed on the top surface of the cylindrical sample [31], using a wet pad to assure good electrical contact. The carbonation of each sample was determined individually by an abrupt increase in the potential (of about 0.2 V) that corresponds to a change in the pH, thus avoiding the possible dispersion in the advance of the carbonation front caused by the placement of samples in the chamber [32].

Carbonated and non-carbonated reinforced samples, all of them chloride contaminated, were exposed to high relative humidity (92–93%) at room temperature for 8 years. That is to say, they were exposed to very favorable humidity conditions to induce chloride corrosion [33].

The electrochemical monitoring of the corrosion behavior was carried out using corrosion potential (E_{corr}) and electrochemical impedance spectroscopy (EIS) measurements. To obtain the E_{corr} values, a SCE was used (Fig. 2). For the EIS measurements, a three-electrode configuration was used. The surface of corrugated bar exposed to the mortar acted as the working electrode, the reference electrode was a SCE (Fig. 2) and the counter-electrode was a copper cylinder, with a slightly larger diameter than that of the mortar sample. To assure good contact between the mortar and the counter-electrode, a wet pad was used. The EIS spectra were acquired using a perturbation signal of 10 mV_{rms} of amplitude. The frequency range of the EIS measurements varied from 10^3 to 10^{-3} Hz. Five points per decade were measured.

After an 8-year exposure period, the reinforced mortar samples were submitted to anodic polarization tests. The tests started from the E_{corr} and they were based on short potentiostatic steps of 10 min. When a potential of about 100 mV vs SCE was reached, the length of the steps increased up to 1 h. The increase in the length on the steps was due to higher difficulties of stabilization of the current signal at increasing anodic overpotentials. All the steps (short and long) increased the potential in 20 mV. The polarization steps finished at 900 mV vs. SCE. More information about the anodic polarization tests designed for the reinforced samples can be found in [27]. This method allows discriminating between the influence of the ohmic drop through the mortar cover and the electrochemical process on the surface of the bar.

Non-welded CS bars of 12 mm in diameter were also embedded in mortar and studied in the same way to be used as reference. The chemical composition of these bars can be found in Table 1.

3. Results and discussion

The E_{corr} values measured for the welded bars in non-carbonated and carbonated mortars with chlorides are plotted in Fig. 3. The probability of corrosion deduced from E_{corr} values as it is proposed in the ASTM C876 standard is also plotted in the figure. These ranges have been initially proposed for CS reinforcements, but their utility for stainless steel reinforcements has been recently discussed [27].

It can be seen that similar welded stainless steel bars seem to remain passive in the mortar if it is not carbonated (Fig. 3a). E_{corr} typical of the passive state are measured throughout the exposure, in spite of the adverse effects of the welding process that has been suggested by solution tests [17]. Other authors have reported that welded stainless steel bars became active after a few months of exposure in mortar [10] or in fly-ash activated mortar [34]. The differences between the results in this work and other published data can be explained bearing in mind the importance of the sandblasting process carried out during the present experimentation. Sandblasting has been proved to partially restore the corrosion resistance of welded stainless steels in solution tests [17]. These results suggest that similar welded stainless steels could be embedded in non-carbonated mortar and exposed to chloride-contaminated conditions, if the heat-tints are previously cleaned by sandblasting. In solution tests, a limited efficiency of the cleaning process of the welding oxides for restoring the corrosion resistance of S20430–S20430 has been detected [17]. However, this grade does not spontaneously corrode in non-carbonated mortar with chlorides at high relative humidity.

S30403–S30403 and S32205–S32205 also exhibit E_{corr} typical of the passive state when they are embedded in carbonated mortar with chlorides (Fig. 3b). However, the results are different for S20430–S20430 (Fig. 3b). After about 5 years of exposure, the E_{corr} of S20430–S20430 leaves the region of passivity with a probability

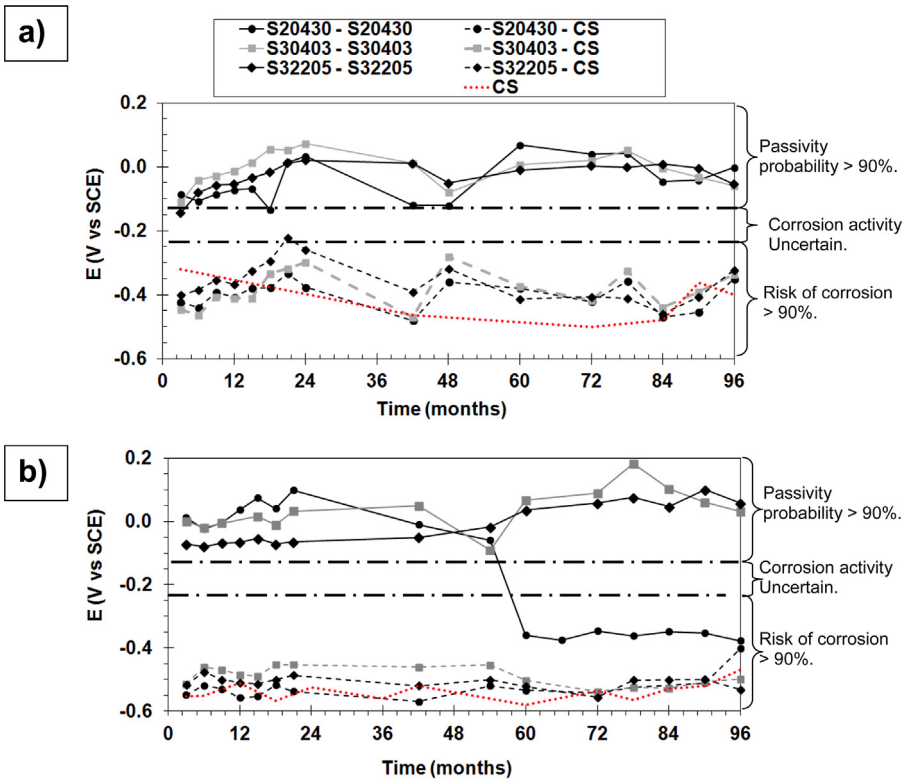

Fig. 3. E_{corr} evolution of the samples during the first 8 years of exposure at high relative humidity (92–93%): (a) non-carbonated mortars; (b) carbonated mortars.

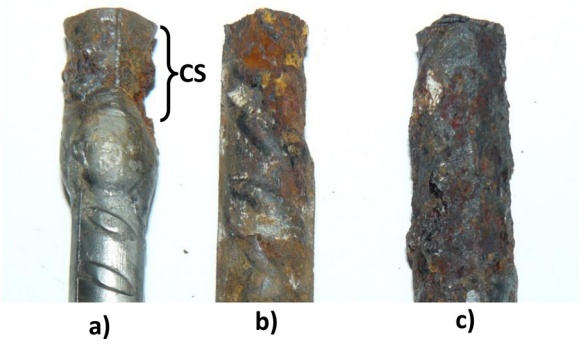

Fig. 4. Attack on CS after the 9 year-tests in different samples: (a) CS welded to stainless steel reinforcements; (b) non-welded CS reinforcement inside non-cracked mortar; (c) non-welded CS reinforcement inside cracked mortar.

higher than 90%, and it is clearly inside the region of corrosion with a probability higher than 90%. The adverse effect of carbonation on the corrosion behavior of welded stainless steel bars is coherent with the results obtained in solution tests [17].

On the other hand, dissimilar welded samples exhibit E_{corr} values typical of the active state since the beginning of the exposure (Fig. 3a and b), independently from the fact whether the mortar is carbonated or not. The visual examination of dissimilar welded bars after the exposure allows checking that there is no sign of corrosion neither on the weld material nor on the stainless steel reinforcement, but that the CS bar is corroded (Fig. 4a). Hence, the low E_{corr} observed during exposure (Fig. 3) have only been caused by the corrosion of the CS bars that have polarized all the reinforcement in the negative direction. It can be pointed out that, in the literature, the critical chloride threshold for CS has been established between 0.9 and 1.4% by weight of cement [35]. Samples analyzed in this work have 1.9% of Cl by weight of cement, so they clearly surpassed this threshold.

Non-welded CS samples show active E_{corr} values during all the exposure (Fig. 3a and b). If the E_{corr} of welded and non-welded CS are compared, no meaningful anodic polarization of the CS can be detected due to the dissimilar welding. Moreover, dissimilar welded samples do not show visible cracks in mortar during the 8-year monitoring period, while most of the non-welded CS samples start to crack in few months. The visual examination of non-welded CS bars embedded in non-cracked mortar after the whole exposure (Fig. 4b) suggests a higher intensity of the attack than that observed on the welded CS (Fig. 4a). Obviously, in cracked samples, where CS has been exposed directly to the air, the corrosion is more severe (Fig. 4c).

The EIS spectra corresponding to passive similar welded stainless steel reinforcements (accordingly to E_{corr}, Fig. 3) have shapes like those shown in the example in Fig. 5a. The spectra obtained during all the exposure for these samples are always simulated using the equivalent circuit in Fig. 5b. Fitted curves obtained for the experimental data using this circuit has been included in Fig. 5a. The equivalent circuit in Fig. 5b, with 2 time constants, has previously proved to be adequate to fit the impedance spectra of stainless steel bars in alkaline solutions [1,2,4]. It has also been used to simulate the behavior of non-welded stainless steel reinforcements in mortar when the system was passive [27]. Although other circuits have also been proposed for similar systems in the literature [23], this one has been considered the most adequate by the authors.

In the circuit in Fig. 5b, constant phase elements (CPE) have been used to simulate the capacitive behaviors. R_m has been identified with the ohmic drop that occurs in the mortar, R_{pl} and CPE_{pl} with the resistance of the passive layer and its capacitive behavior, respectively, and R_t and CPE_{dl} with the charge transfer resistance and the capacitive behavior of the double layer, respectively.

On the other hand, the EIS spectra corresponding to the dissimilar welded bars are different (see example in Fig. 6a). To obtain an adequate fitting in these cases, a Warburg element must be included in the 2 time-constant, hierarchic equivalent circuit,

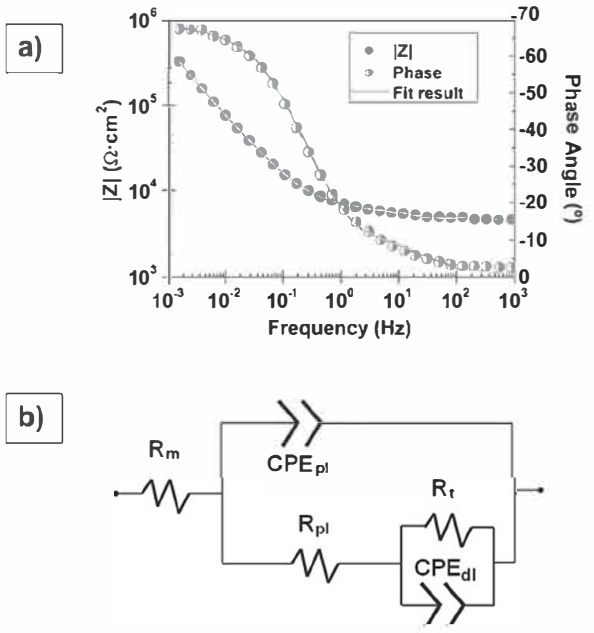

Fig. 5. (a) Example of the EIS spectra obtaining for similar welded stainless steel bars whose E_{corr} are in the passive region (data corresponding to S20430–S20430 after 6 months of exposure in non-carbonated mortar); (b) equivalent circuit used to fit all the spectra corresponding to passive similar welded stainless steel bars.

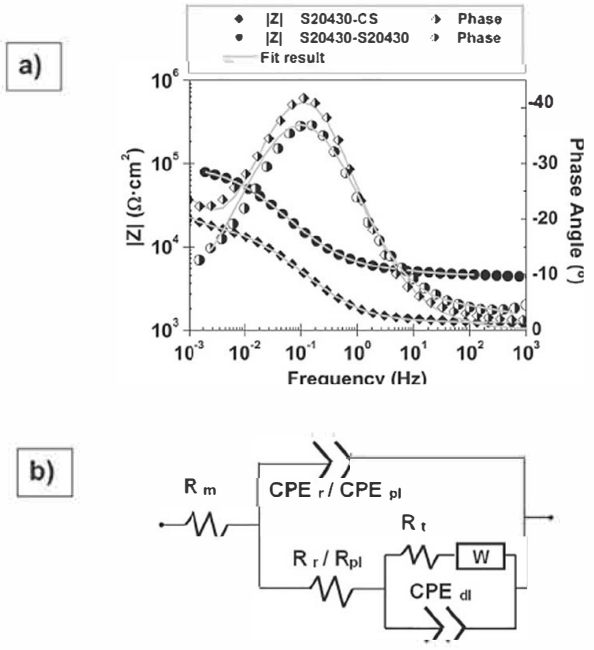

Fig. 6. (a) Example of the EIS spectra obtained for active welded bars (data corresponding to S20430-CS after 6 months of exposure in non-carbonated mortar and S20430–S20430 after 60 months of exposure in carbonated mortar); (b) equivalent circuit used to fit all the spectra corresponding to active welded bars.

resulting in the circuit in Fig. 6b. Other authors testing CS bars in solution have included the Warburg element [36], and a circuit similar to that in Fig. 6b has been used. The influence of the transport phenomenon (which is what a Warburg element represents) is easy to understand when the charge transfer step takes place at meaningful rates, and it should be borne in mind that the present testing conditions are very aggressive. Though the relationship between the Warburg impedance and the diffusion of the oxide species for corroding steel in concrete has also been suggested by some authors [37], the Warburg impedance is often identified with

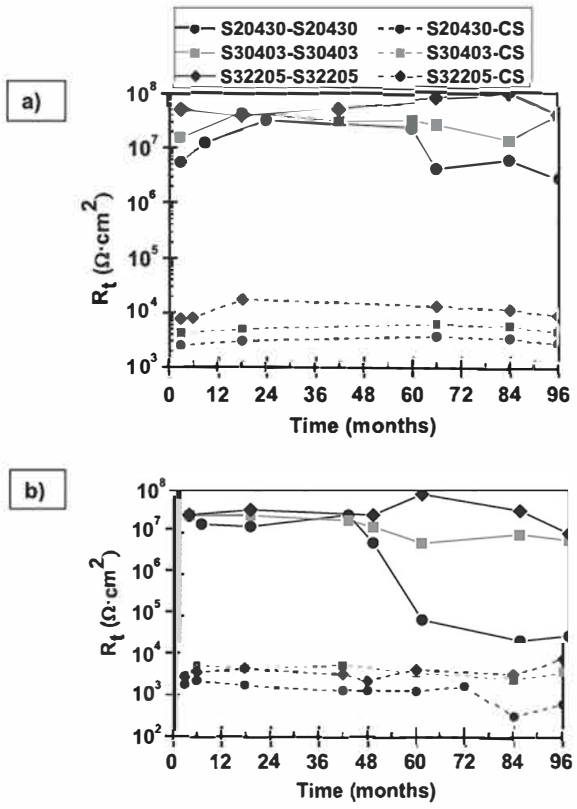

Fig. 7. Time evolution of the R_t values obtained from the analysis of the EIS spectra of welded stainless steels: (a) embedded in non-carbonated mortar; (b) embedded in carbonated mortar.

oxygen diffusion. It is proven that oxygen diffusion is a key factor that can determine the corrosion rate of CS reinforcements at 95% HR or in submerged structures [38]. As the present tests are carried out at high relative humidity (close to 95%), the O_2 diffusion influence in the low-frequency region of the impedance spectra can be expected.

The lowest-frequency time-constant in Fig. 6b (that for stainless steel has been identified with the passive layer influence), for samples with corroding CS—where the passive layer is totally destroyed (Fig. 4), can be better identified with the influence of the rust layer formed on the surface of the CS bars. Hence, R_r and CPE_r in circuit in Fig. 6b are used to simulate the resistance and the capacitive behavior of the rust layer in CS. Bearing in mind the results of the visual observation of the reinforcements after the tests, the parameters obtained from the EIS spectra have been normalized using only the exposed surface of CS and not the whole metallic surface exposed inside the mortars.

Moreover, the circuit in Fig. 6b is also useful to simulate the behavior of similar welded stainless steels whose E_{corr} is in the active region (as the example in Fig. 6a corresponding to S20430–S20430 in carbonated mortar exposed for 60 months, whose E_{corr} can be checked in Fig. 3b). In this case, the lowest-frequency time-constant (for similar welded stainless steel, R_{pl} and CPE_{pl}) in circuit in Fig. 6b could be better identified with the passive layer remaining on the surface of the welded stainless steel.

Usually, one of the most meaningful parameters that can be obtained from the EIS analysis is the R_t value. The R_t corresponding to similar welded and dissimilar welded stainless steel reinforcements embedded in non-carbonated mortar are shown in Fig. 7a. For similar welded stainless steels, the R_t exhibits values characteristic of stainless steel reinforcements in passive state [27]. Those values are obtained by extrapolation of the experimental spectra to very-low frequencies, so they imply a high uncertainty about their

exact value. However, they are relevant as they allow to assure that similar welded stainless steels do not suffer any kind of corrosive attack during the testing period when they are embedded in non-carbonated mortar with chlorides.

When dissimilar welded stainless steels are embedded in non-carbonated mortar (Fig. 7a), the R_t values are much lower, suggesting active corrosion. All these results are coherent with the information deduced from the E_{corr} values in Fig. 3a.

The R_t values corresponding to the welded samples in carbonated mortar are plotted in Fig. 7b. S30403–S30403 and S32205–S32205 exhibit high R_t values throughout the exposure, confirming their passivity. On the other hand, a marked decrease on the R_t for S20430–S20430 is observed after 60 months, coinciding with the E_{corr} leaving the passivity region (Fig. 3b). These low R_t values, typical of active state, can be calculated with much more precision as their influence appears in frequency regions of the spectra where experimental data exists.

Dissimilar welded steels embedded in carbonated mortar (Fig. 7b) show R_t values that tend to be slightly lower than those of the same reinforcements in non-carbonated mortar. This is coherent with the higher aggressivity of chlorides in mortars with lower pH. Carbonation fosters the chloride attack on the CS bars. Anyway, it is worth pointing out that R_t values obtained for dissimilar welded stainless steels (that is to say, for sandblasted CS) are always lower than those calculated for corroding S20430–S20430 in carbonated mortar.

Some examples of other data obtained from the EIS spectra of the similar welded stainless steel reinforcements are shown in Table 2. The C_{dl} values shown in Table 2 are similar or very close to the typical capacitances of those associated to a charge transfer step of passive steel-concrete systems [39,40].

It can also be seen that R_m and R_{pl} in Table 2 exhibit values that are orders of magnitude lower than R_t (Fig. 7). That is to say, the charge transfer is the rate-limiting step for passive reinforcements. This fact also allows us to identify R_t with the polarization resistance in the Stern–Geary equation [41] and calculate corrosion intensities (i_{corr}). A Stern–Geary constant (B) value of 48–53 mV has been determined for stainless steel in alkaline media [5]. Then, the i_{corr} for similar welded stainless steels in non-carbonated mortar with chlorides would be about nA/cm^2. It is obvious that these i_{corr} are able to comply with any durability requirement of reinforced structures, in spite of the suggested adverse effect of the weldings on the stability of the passivity [17].

Examples of other results different from R_t obtained from the simulation of the EIS spectra of the dissimilar welded bars can be seen in Table 3, being the impedance results completely dominated by the response of CS. The values obtained from the simulation to capacitive behavior of the rust layer shows a much higher dispersion than those found for the capacitive behavior of the passive layer (Table 2). This can be easily understood bearing in mind the much more heterogeneous, unstable structure and morphology that the rust layers should have. The obtained R_r values (Table 3) are lower than those shown in Table 2 for R_{pl}, as expected. The high C_{dl} and low n_{dl} values are typical of CS corroding at a high rate in concrete, as other authors have previously reported [39,42].

In Table 3, values for R_r and R_m are lower than R_t (Fig. 7), but clearly not negligible. The influence of the value determined for R_m on the development of the corrosion process is not easy to extrapolate. The R_m measured is the resistance through the mortar thickness surrounding the metallic reinforcement (Fig. 2), but the mortar resistance that can cause a decrease in the corrosion rate is that corresponding to mortar volume existing between the anodes and the cathodes that form the corrosion cells on the reinforcement surface. It can be assumed that this resistance could be lower than the measured R_m. Anyway, the influence of R_r on the calculus of the global corrosion rate should not be omitted in these cases.

Table 2
Values for R_m, R_{pl}, C_{pl}, n_r, C_{dl} and n_{dl} obtained from the analysis of the EIS spectra of similar welded stainless steels embedded in non-carbonated and carbonated mortar with chlorides.

Similar welded grade	Exposure time (months)	Non carbonated						Carbonated					
		R_m (kΩ cm^2)	C_{pl} (μF cm^{-2} s^{n-1})	n_{pl}	R_{pl} (kΩ cm^2)	C_{dl} (μF cm^{-2} s^{n-1})	n_{dl}	R_m (kΩ cm^2)	C_{pl} (μF cm^{-2} s^{n-1})	n_{pl}	R_{pl} (kΩ cm^2)	C_{dl} (μF cm^{-2} s^{n-1})	n_{dl}
S20430–S20430	3	0.9	50	0.82	0.4	85	0.83	2.9	29	0.85	1.7	37	0.84
	18	3.7	9	0.83	0.4	94	0.81	3.6	38	0.84	4.4	27	0.83
	66	8.6	25	0.79	4.1	76	0.80	4.5	29	0.75	1.4	70	0.76
	84	7.8	20	0.81	3.5	80	0.79	2.2	72	0.73	1.5	82	0.75
	96	5.5	22	0.80	2.7	87	0.75	3.4	43	0.75	1.9	80	0.80
S30403–S30403	3	2.1	88	0.82	13.4	14	0.85	2.2	30	0.86	1.4	41	0.86
	18	8.2	37	0.82	11.4	48	0.81	4.3	18	0.85	1.0	45	0.85
	66	14.9	15	0.75	29.2	53	0.76	3.2	32	0.78	4.8	35	0.81
	84	13.0	22	0.76	31.7	59	0.81	2.3	20	0.79	1.8	50	0.79
	96	9.2	19	0.79	17.1	74	0.79	10.6	8	0.89	10.0	14	0.78
S32205–S32205	3	1.1	68	0.98	1.1	51	0.76	3.4	25	0.82	3.2	43	0.82
	18	5.3	39	0.80	5.5	59	0.85	6.6	29	0.80	9.5	30	0.81
	66	7.0	13	0.94	8.4	87	0.81	1.4	46	0.75	12.1	25	0.81
	84	4.4	12	0.94	6.0	98	0.81	1.1	33	0.75	3.6	45	0.78
	96	4.5	13	0.92	6.4	90	0.81	6.7	11	0.79	31.4	12	0.75

Table 3
Values for R_m, R_r, C_r, n_r, C_{dl} and n_{dl} obtained from the analysis of the EIS spectra of dissimilar welded stainless steels embedded in non-carbonated and carbonated mortar with chlorides.

Dissimilar welded grades	Exposure time(months)	Non carbonated						Carbonated					
		R_m (kΩ cm^2)	C_r (μF cm^{-2} s^{n-1})	n_r	R_r (kΩ cm^2)	C_{dl} (μF cm^{-2} s^{n-1})	n_{dl}	R_m (kΩ cm^2)	C_r (μF cm^{-2} s^{n-1})	n_r	R_r (kΩ cm^2)	C_{dl} (μF cm^{-2} s^{n-1})	n_{dl}
S20430-CS	3	0.84	95	0.95	0.3	249	0.71	0.83	60	0.51	0.20	835	0.54
	18	1.21	35	0.90	0.3	249	0.74	1.42	178	0.58	0.25	854	0.61
	60	2.67	21	0.90	0.1	222	0.71	0.45	528	0.69	0.41	1889	0.59
	84	4.83	59	0.80	1.3	132	0.71	0.71	1663	0.54	0.28	2600	0.75
	96	3.82	34	0.80	0.9	184	0.73	0.68	1322	0.52	1.46	4141	0.73
S30403-CS	3	0.83	190	0.88	1.0	248	0.80	1.88	269	0.56	0.15	289	0.60
	18	2.02	4	0.57	0.5	221	0.60	2.78	248	0.55	1.68	248	0.72
	60	3.41	17	0.53	1.0	108	0.60	0.80	257	0.60	2.55	1247	0.85
	84	2.44	103	0.51	1.1	54	0.60	0.82	323	0.59	1.82	1625	0.85
	96	2.01	48	0.58	1.0	77	0.60	1.33	176	0.74	1.27	710	0.52
S32205-CS	3	0.88	194	0.90	1.2	116	0.62	2.48	218	0.90	0.24	607	0.60
	18	4.17	95	0.70	1.5	129	0.85	3.65	104	0.53	0.78	287	0.63
	60	5.95	72	0.70	2.5	226	0.74	0.29	3	0.54	0.39	547	0.57
	84	5.68	107	0.55	1.5	192	0.76	0.91	33	0.60	0.15	743	0.56
	96	5.73	110	0.59	2.7	196	0.81	3.88	118	0.73	6.20	213	0.96

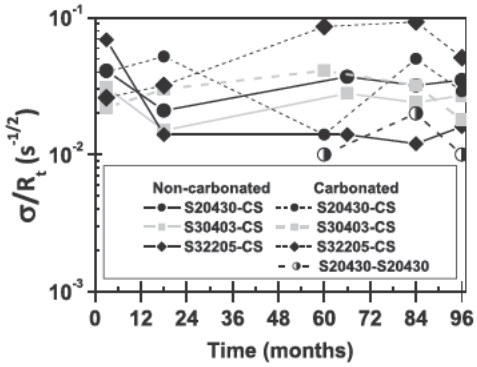

Fig. 8. Ratio between σ values (related to the O_2 diffusion impedance) and R_t values, both obtained from the analysis of the EIS spectra of active welded reinforcements.

Another parameter than can sometimes exert an important influence on the corrosion kinetic of corroding reinforcements is the Warburg coefficient (σ). σ is related to diffusion of the species involved in the corrosive attack. Though minor discrepancies can be found in the literature regarding the relationship between σ and the Nernst diffusion layer thickness [43], in this case, semi-infinite diffusion can be assumed. The effect of the diffusion appears on the spectra of active samples (Fig. 6a). A higher value of σ implies higher diffusion impedance, and thus, a higher influence of the diffusion step on the control of the corrosion rate. A certain uncertainty associated to the values obtained for this parameter can be understood bearing in mind that the influence of the diffusion appears in the very low frequency region of the spectrum. σ values are mainly obtained by extrapolation from points that already have a small experimental error.

The σ/R_t values for the welded CS bars and active S20430–S20430 are plotted in Fig. 8. σ/R_t ratio has been used to estimate which step determines the corrosion rate (diffusion or charge transfer) [44]. For dissimilar welded steels in non-carbonated mortars, σ/R_t ratios range from 0.01 to 0.04 $s^{-1/2}$. The σ/R_t values obtained allow to know that diffusion is not the corrosion rate controlling step for those CS bars and the influence of the diffusion on the corrosion rate can be considered negligible for these cases, as the ratios are always much lower than 1. However, it should be pointed out that the increase of σ randomly observed during the last stage of the exposure of carbonated samples suggests that, under those circumstances, the diffusion impedance could exert a certain influence on the control of the corrosion rate, always being lower than the influence of the charge transfer step. For these cases, a mixed control of the corrosion rate could be assumed, being the charge transfer step the most influencing one. The increase of the diffusion impedance could be related to a partial blocking of the pores by the corrosion products. Steel in carbonated mortar corrodes at a higher rate and, the lower porosity of carbonated samples (due to the precipitation of $CaCO_3$ inside the pores, [45]) can promote the corrosion products to exert a more noticeable influence on the diffusion impedance than on the non-carbonated samples.

Hence, it is clear that the corrosion rate is mainly controlled by the charge transfer step, but other resistances causing ohmic drop (and sometimes also the Warburg impedance) could contribute to slightly decrease the corrosion rate of welded CS bars. That is to say, the polarization resistance can be considered slightly higher than R_t. Assuming B values about 26 mV [40], approximated i_{corr} values for the welded CS between 1 and 10 μA/cm^2 could be estimated. The corrosion rates in non-carbonated mortar are in the lowest part of this range, while those calculated for reinforcements in carbonated mortar are in the highest part. It should be borne in mind that

i_{corr} >1 μA/cm^2 should be considered as heavy corrosion, following the RILEM recommendations [46].

S20430–S20430 in carbonated mortar is active during the last years of exposure (Figs. 3 b and 7 b). As in this case the σ/R_t is about 0.01 $s^{-1/2}$ (Fig. 8), the influence of the diffusion step on the corrosion rate can be considered as negligible, and the corrosion rate is controlled by charge transfer step. A polarization resistance of $3 \times 10^5\ \Omega \times cm^2$ has been previously suggested to discriminate between active and passive CS reinforcements [13]. The values obtained for this R_t after 5 year of exposure are below this value. If R_t is identified to the polarization resistance, the active state of the system will be confirmed. Assuming B values about 26 mV, as it has been traditionally done for active steel in concrete [40], i_{corr} of approximately 0.5 μA/cm^2 could take place. For steel in concrete, these i_{corr} values would correspond to low-moderate corrosion [46]. The corrosion rates of S20430–S20430 in carbonated mortar at the end of the exposure are lower than those estimated for welded CS.

The EIS spectra corresponding to the non-welded CS bars are mainly dominated by the resistive behavior of the mortar. Moreover, when cracks appear the mortar, they partially disrupt the propagation of the electrical signal in some regions and probably caused big heterogeneities in the development of the corrosion process. The blocking of the pores by the corrosion products can also contribute to the anomalies in the electric signal propagation. These distorted spectra are typical of steels that have been corroding at a high rate for a long time in mortar or concrete [47]. The only meaningful information that can be obtained from them is that the resistances associated to the corrosion process are lower than R_m (that is about 4–7 kΩ cm^2).

This data confirm the information suggested in Fig. 4 about the beneficial effect of welding and sandblasting on the corrosion rate of CS, as information about the corrosion process can be obtained from the EIS spectra of welded CS but not from non-welded CS. The strength of the galvanic couple formed by stainless steel and CS in mortar has been reported as negligible [11,12], as mentioned previously. Moreover, a potentially weak effect of the stainless steel on the corrosion rate of the CS can be masked by the beneficial effect of the sandblasting. Several authors have reported that sandblasted CS bars exhibit higher chloride-threshold levels than those in as-received (mill-scaled) conditions [48,49]. The presence of mill-scale damages the protective characteristics of the passive layer [50] and, if the CS is severely pre-rusted, the passivity can be totally inhibited [51].

Anodic polarizations are carried out after 8 years of exposure to obtain additional information about the stability of the aged passive films formed in mortar and their protective ability in the tested conditions. The results of the polarization of the welded reinforcements are plotted as Evans diagrams in Fig. 9. Except S20430–S20430 in carbonated mortar, curves corresponding to similar welded stainless steel are defined at low current densities (typical of a passive state) during a wide range of potentials. Hence, the existence of a stable protective layer on the surface of these samples is confirmed. The oxidation of Cr(III) in the passive layer to Cr(VI) that takes place during the anodic polarization [25] does not allow to observe the high anodic slopes seen in the polarization curves in other passive systems.

Curves corresponding to S20430–S20430 in carbonated mortar and all the curves corresponding to dissimilar welded have the typical shape of the anodic branch of the polarization curve of active systems. This confirms the conclusions about the corrosion activity drawn from the E_{corr} results (Fig. 3) and R_t values (Fig. 7) obtained for all those welded samples at the end of the 8 year exposure.

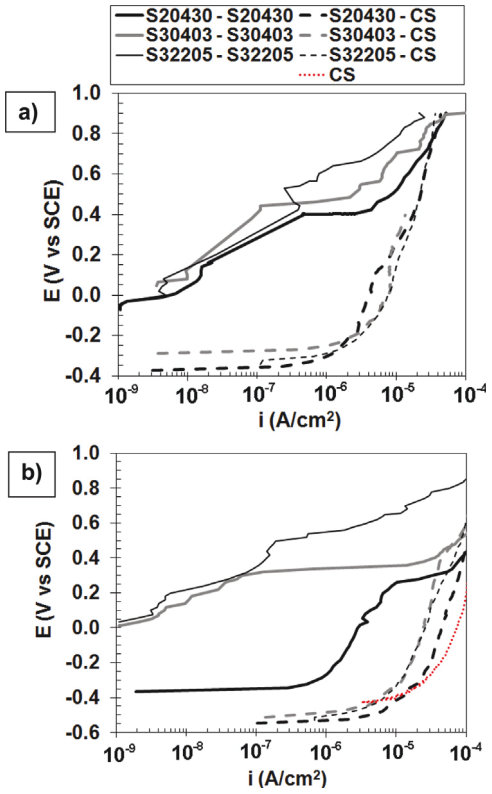

Fig. 9. Anodic polarization curves of the reinforced mortar: (a) non-carbonated mortar; (b) carbonated mortar.

It is also worth pointing out that the current densities defined at low anodic overpotentials for welded CS in non-carbonated mortar (Fig. 9a) are lower than those defined for the same reinforcements in carbonated mortar (Fig. 9b), confirming the information suggested by the R_t about the influence of the mortar pH on the corrosion rate (Fig. 7). Moreover, in carbonated mortar and at potentials close to E_{corr} (Fig. 9b), the curve corresponding to the active S20430–S20430 is shifted to lower current densities than the curves corresponding to welded CS. This is coherent with lower i_{corr} for active S20430–S20430 than for CS welded reinforcements, as EIS results have suggested.

In Fig. 9b, information corresponding to a non-cracked sample with non-welded CS has been included. The intensities observed for non-welded CS at small anodic polarizations are about one order of magnitude higher than those for welded CS in the same conditions. This seems to confirm again the positive effect of sandblasting on the corrosion behavior of CS.

In order to easily visualize the relative stability of the passive systems studied, the anodic potentials corresponding to current densities of 2×10^{-6} A/cm^2 of the curves in Fig. 9 have been plotted in Fig. 10. This criterion has been used in previous research [27] with the same aim. Results of non-welded materials submitted to similar tests [27,52] have also been included in the figure for

Table 4
Localization of the pits after the testing in similar welded stainless steels.

Chloride contaminated mortar	S20430	S30403	S32205
Non-carbonated	Corrugated bar	Corrugated ba + weld material	Weld material
Carbonated	Corrugated bar + weld material	Corrugated bar + weld material	Weld material

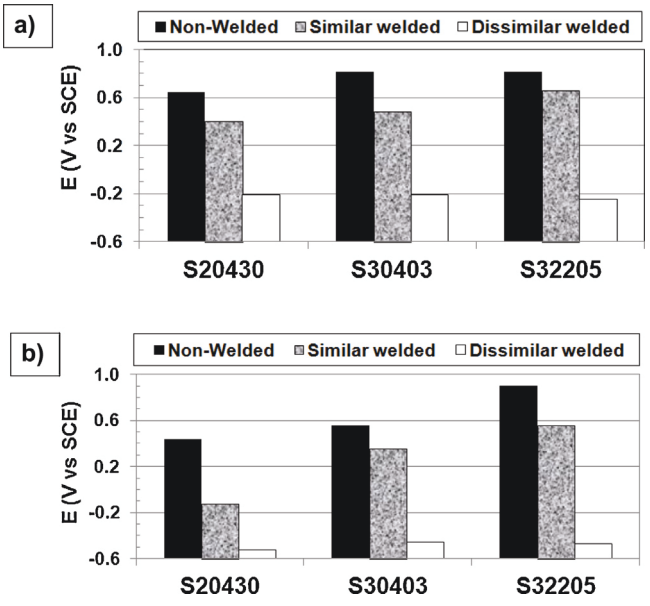

Fig. 10. Potentials needed to reach an anodic current density of 2×10^{-6} A/cm^{-2} for reinforcements embedded for 8 years in mortar with chlorides at high relative humidity (92–93%): (a) non-carbonated mortar; (b) carbonated mortar.

comparison. Similar welded stainless steels need anodic polarizations to corrode at high rate that are proportional to their corrosion resistance when they are non-welded [17]. The pitting resistance of the welded reinforcements is conditioned by the alloying degree of the stainless steels. Polarization tests in mortar show a certain decrease in the length of the passive regions of similar welded stainless steel in comparison to the non-welded bars in similar conditions, in spite of the sandblasting.

Dissimilar welded bars exhibit the same results in Fig. 10, independently from the composition of the stainless steels, but there are clear differences due to the pH of the mortar. The adverse effect of carbonation on corrosion behavior is again confirmed, not only when general corrosion takes place, but also when corrosion proceeds in a generalized way (Fig. 4).

After being polarized, the mortar samples continued their exposure at high relative humidity for 1 year. During this period, the attack caused by anodic polarization was allowed to grow and to become clearly detectable. After breaking the mortar samples and cleaning the reinforcements, it could be checked that all similar welded stainless steels corrode by pitting (Table 4), while in those welded to CS, only the CS is attacked and the attack is completely general (Fig. 4a). Hence, a certain cathodic protection of the stainless steels caused by their welding to CS can be assumed.

S32205–S32205 only pits in the weld material (Table 4). So, the corrugated surfaces of S32205 have very good behavior in spite of the high polarizations they have been submitted to (Fig. 9) and the aggressivity of the exposure. The weld electrode used for S32205 is one of the recommended by the manufacturers and used habitually for this grade. However, in these alkaline conditions, it has a lower corrosion resistance than the S32205. The corrosion resistance of S32205–S32205 is very high and can fulfill any service requirement, but it could be improved even further by using a more alloyed welding electrode.

On S30403–S30403, pits appear on the corrugated bar as well as on the weld material, so both have similar corrosion resistance in mortar. The results in Fig. 10 comparing non-welded S30403 and S30403–S30403 reflect the decrease in the corrosion resistance caused by the surface modifications due to sandblasting (Fig. 1). The embedded sand particles can introduce stresses in the surface material and create crevices [17]. Results in Table 4 corresponding to S20430–S20430 suggest that the decrease in its corrosion resistance in comparison to the non-welded grade is also due to secondary effects of the cleaning.

4. Conclusions

1. If the heat-tints are previously cleaned by sandblasting, welded stainless steels could be embedded in non-carbonated mortar and exposed to chloride-contaminated conditions and high relative humidity (92–93%).
2. Sandblasted S20430–S20430 corrodes spontaneously in carbonated mortar with chlorides after a few years of exposure.
3. Welded, sandblasted stainless steel reinforcements have lower corrosion resistance than non-welded stainless steels with the same composition.
4. The effect of sandblasting is beneficial for the CS, as it reduces the corrosion rate. The possible increase of the corrosion rate of CS due to the galvanic couple formed with the stainless steels during welding is masked by the sandblasting.
5. The corrosion resistance of sandblasted duplex S32205–S32205 is very good, but it could be improved even further by using a more alloyed welding electrode than the one used in the present research.

Acknowledgement

The present work was funded by the Spanish Ministry of Science and Innovation through the Project reference BIA2007-66491-C02-02.

References

[1] A. Bautista, G. Blanco, F. Velasco, A. Gutiérrez, L. Soriano, F.J. Palomares, H. Takenouti, Changes in the passive layer of corrugated, low Ni, austenitic stainless steel due to the exposure to simulated pore solutions, Corros. Sci. 51 (2009) 785–792.
[2] H. Luo, C.F. Dong, X.G. Li, K. Xiao, The electrochemical behavior of 2205 duplex stainless steel in alkaline solutions with different pH in presence of chlorides, Electrochim. Acta 64 (2012) 211–220.
[3] B. Elsener, D. Addari, S. Coray, A. Rossi, Nickel-free manganese bearing stainless steel in alkaline media—electrochemistry and surface chemistry, Electrochim. Acta 56 (2011) 4489–4497.
[4] L. Freire, M.J. Carmenzim, M.G.S. Ferreira, M.F. Montemor, The electrochemical behavior of stainless steel AISI 304 in alkaline solution with different pH in presence of chlorides, Electrochim. Acta 56 (2011) 5280–5289.
[5] S. Fajardo, D.M. Bastidas, M. Criado, J.M. Bastidas, Electrochemical study of the corrosion behaviour of a new low nickel stainless steel in carbonated alkaline solution in presence of chlorides, Electrochim. Acta 129 (2014) 160–170.
[6] S.M. Alvarez, A. Bautista, F. Velasco, Influence of strain-induced martensite in the anodic dissolution of austenitic stainless steels in acid medium, Corros. Sci. 59 (2013) 130–138.
[7] A. Bautista, S.M. Alvarez, F. Velasco, Selective corrosion of duplex stainless steel bars in acid. Part II: effect of the surface strain and numerical analysis, Mater. Corros. 66 (2015) 357–365.
[8] E.C. Paredes, A. Bautista, S.M. Alvarez, F. Velasco, Influence of the forming process of corrugated stainless steels on their corrosion behaviour in simulated pore solutions, Corros. Sci. 58 (2012) 52–61.
[9] X. Feng, X. Lu, Y. Zuo, D. Chen, The passive behavior of 304 stainless steel in saturated calcium hydroxide solution under different deformations, Corros. Sci. 82 (2014) 347–355.
[10] M.C. García-Alonso, J.A. González, J. Miranda, M.L. Escudero, M.J. Correia, M. Salta, A. Bennani, Corrosion behaviour of innovative stainless steels in mortar, Cem. Concr. Res. 37 (2007) 1562–1569.
[11] J.T. Pérez-Quiroz, J. Terán, M.J. Herrera, M. Martínez, J. Genesca, Assessment of stainless steel reinforcement for concrete structures rehabilitation, J. Constr. Steel Res. 64 (2008) 1317–1324.
[12] L. Bertolini, P. Pedeferri, Laboratory and field experience on the use of stainless steels to improve the durability of reinforced concrete, Corros. Rev. 20 (2011) 129–152.
[13] M. Serdar, L. Valek Žulj, D. Bjegović, Long-term corrosion behavior of stainless reinforcing steel in mortar exposed to chloride environment, Corros. Sci. 69 (2013) 149–157.
[14] M.R. Valluzzi, L. Binda, C. Modena, Mechanical behaviour of historic masonry structures strengthened by bed joints structural repointing, Constr. Build. Mater. 19 (2005) 63–73.

[15] M.D. Lepech, M. Geiker, H. Stang, Probabilistic design and management of environmentally sustainable repair and rehabilitation of reinforced concrete structures, Cem. Concr. Comp. 47 (2014) 19–31.
[16] F. Velasco, G. Blanco, A. Bautista, M.A. Martínez, Effect of welding on local mechanical properties of stainless steels for concrete structures using universal hardness tests, Constr. Build. Mater. 23 (2009) 1883–1891.
[17] A. Bautista, G. Blanco, F. Velasco, M.A. Martinez, Corrosion performance of welded stainless steel reinforcements in simulated pore solutions, Constr. Build. Mater. 21 (2007) 1267–1276.
[18] L. Li, C.F. Dong, K. Xiao, J.Z. Yao, X.G. Li, Effect of the pH on pitting corrosion of stainless steel welds in alkaline salt water, Const. Build. Mater. 68 (2014) 709–715.
[19] G. Hinds, L. Wickström, K. Mingard, A. Turnbull, Impact of surface condition on sulphide stress corrosion cracking of 316L stainless steel, Corros. Sci. 71 (2013) 43–52.
[20] B. Kurt, A. Çalik, Interface structure of diffusion bonded duplex stainless steel and medium carbon steel couple, Mater. Charact. 60 (2009) 1035–1040.
[21] I. Esih, V. Alar, I. Juraga, Influence of thermal oxides on pitting corrosion of stainless steel in chloride solutions, Corros. Eng. Sci. Technol. 40 (2005) 110–120.
[22] E.I. Moreno, P. Castro-Borgues, A.A. Torres-Acosta, A. Cárdenas, O. Tronconis de Rincón, Chloride analysis in a 62-year old concrete pier reinforced with type 304 bars, in: NACE Corrosion Conference, 11–15 March 2007, Nashville, Tennessee, 2015, paper 07240.
[23] R.G. Duarte, A.S. Castela, R. Neves, L. Freire, M.F. Montemor, Corrosion behavior of stainless steel rebars embedded in concrete: an electrochemical impedance spectroscopy study, Electrochim. Acta 124 (2014) 218–224.
[24] A. Bautista, G. Blanco, F. Velasco, Corrosion behaviour of low-nickel austenitic stainless steel reinforcements: a comparative study in simulated pore solutions, Cem. Concr. Res. 36 (2006) 1922–1930.
[25] S.M. Alvarez, A. Bautista, F. Velasco, Corrosion behaviour of corrugated lean duplex stainless steels in simulated concrete pore solutions, Corros. Sci. 53 (2011) 1748–1755.
[26] A. Poursaee, C.M. Hansson, Reinforcing steel passivation in mortar and pore solution, Cem. Concr. Res. 37 (2007) 1127–1133.
[27] A. Bautista, E.C. Paredes, F. Velasco, S.M. Alvarez, Corrugated stainless steels embedded in mortar for 9 years: corrosion results of non-carbonated, chloride-contaminated samples, Constr. Build. Mater. 93 (2015) 350–359.
[28] I. Fayala, L. Dhouibi, X.R. Nóvoa, M. Ben Ouezdou, Effect of inhibitors on the corrosion of galvanized steel and on mortar properties, Cem. Concr. Comp. 35 (2013) 181–189.
[29] O. Oueslati, J. Duchesne, The effect of SCMs on the corrosion of rebar embedded in mortars subjected to an acetic acid attack, Cem. Concr. Res. 42 (2012) 467–475.
[30] P.K. Mehta, P.J.M. Monteiro, Concrete: Microstructure, Properties and Materials, second ed., Prentice Hall, Englewood Cliffs, New Jersey, 1993.
[31] P. Castro, A.A. Sagües, E.I. Moreno, L. Maldona, J. Genescá, Characterization of activated titanium solid reference electrodes for corrosion testing of steel in concrete, Corrosion 52 (1996) 609–617.
[32] K. Kinoshita, M.J. Madou, Electrochemical measurements on Pt, Ir, and Ti oxides as pH probes, J. Electrochem. Soc. 131 (1984) 1089–1094.
[33] P. Schiessl, S. Lay, Influence of concrete composition, in: H. Böhni (Ed.), Corrosion in Reinforced Concrete Structures, Woodhead Publishing Limited, Cambridge, 2005, pp. 91–104.
[34] M. Criado, D.M. Bastidas, S. Fajardo, A. Fernández-Jiménez, J.M. Bastidas, Corrosion behaviour of a new low-nickel stainless steel embedded in activated fly ash mortars, Cem. Concr. Comp. 33 (2011) 644–652.
[35] U. Angst, B. Elsener, C.K. Larsen, O. Vennesland, Critical chloride content in reinforced concrete—a review, Cem. Concr. Res. 39 (2009) 1122–1138.
[36] R. Liu, L. Jiang, J. Xu, C. Xiong, Z. Song, Influence of carbonation on chloride-induced reinforcement corrosion in simulated concrete pore solutions, Constr. Build. Mater. 56 (2014) 16–20.
[37] T. Eichler, B. Isecke, R. Bäβler, Investigations on the re-passivation of carbon steel in chloride containing concrete in consequence of cathodic polarization, Mater. Corros. 60 (2009) 119–129.
[38] R.R. Hussai, Effect of moisture variation on oxygen consumption rate of corroding steel in chloride contaminated concrete, Cem. Concr. Comp. 33 (2011) 154.
[39] N. Birbilis, K.M. Nairn, M. Forsuth, On the electrochemical response and interfacial properties of steel-Ca$(OH)_2$ and steel concrete system measured using galvanostatic pulses, Electrochim. Acta 49 (2004) 4331–4339.
[40] G.K. Glass, C.L. Page, N.R. Short, J.-Z. Zhang, The analysis of potentiostatic transients applied to the corrosion of steel in concrete, Corros. Sci. 39 (1997) 1657–1663.
[41] M. Stern, A. Geary, Electrochemical polarization. I. A theoretical analysis of the shape of the polarization curves, J. Electrochem. Soc. 104 (1957) 56–58.
[42] S.-G. Dong, C.-J. Lin, R.-G. Hu, L.-Q. Li, R.-G. Du, Effective monitoring of corrosion in reinforcing steel in concrete constructions by a multifunctional sensor, Electrochim. Acta 56 (2011) 1881–1888.
[43] S.R. Taylor, E. Gileadi, Physical interpretation of the Warburg impedance, Corros. Sci. 51 (1995) 664–671.
[44] V. Feliu, J.A. González, C. Andrade, S. Feliu, Equivalent circuit for modelling the steel–concrete interface. I. Experimental evidence and theoretical predictions, Corros. Sci. 40 (1998) 975–993.
[45] M. Castellote, L. Fernandez, C. Andrade, C. Alonso, Chemical changes and phase analysis of OPC pastes carbonated at different CO_2 concentrations, Mater. Struct. 42 (2009) 515–525.
[46] C. Andrade, C. Alonso, Test methods for in-site corrosion rate measurement for steel reinforcement in concrete by means of the polarization method, Mater. Struct. 37 (2004) 623–643.
[47] R. Vedalakshmi, N. Palaniswamy, Analysis of the electrochemical phenomenon at the rebar–concrete interface using electrochemical impedance spectroscopic technique, Mag. Concr. Res. 62 (2010) 177–189.
[48] T.U. Mohammed, H. Hamada, Corrosion of steel bars in concrete with various steel surface conditions, ACI Mater. J. 103 (2006) 233–242.
[49] M. Manera, O. Vennesland, L. Bertolini, Chloride threshold for rebar corrosion in concrete with addition of silica fume, Corros. Sci. 50 (2008) 554–560.
[50] E. Mahallati, M. Saremi, An assessment in the mill scale effects in the electrochemical characteristics of the bars under DC-polarization, Cem. Concr. Res. 36 (2006) 1324–1329.
[51] J.A. González, E. Ramírez, A. Bautista, S. Feliu, The behaviour of pre-rusted steel in concrete, Cem. Concr. Res. 26 (1996) 501–511.
[52] A. Bautista, S.M. Alvarez, E.C. Paredes, F. Velasco, S. Guzman, Corrugated stainless steels embedded in carbonated mortars with and without chlorides: 9-year corrosion results, Constr. Build. Mater. 95 (2015) 186–196.